

X-ray scattering study of the critical correlation scaling function for a binary liquid mixture

Yoshinobu Izumi

Department of Polymer Science, Faculty of Science, Hokkaido University, Sapporo 060, Japan

(Received 19 July 1988)

A new method for evaluating the critical exponent η and the critical correlation scaling function of a binary liquid mixture is presented by using small-angle x-ray scattering. The new procedure has the benefit that it is free from the uncertainties in collimation corrections, the effects of the cross-section factor, and the cell size used. The procedure was applied to the measurement and analysis of a binary critical mixture of perfluoromethyl-cyclohexane and *n*-heptane. The experimental data agree with the theory of Bray within experimental error [Phys. Lett. A **55**, 453 (1976); Phys. Rev. Lett. **36**, 285 (1976); Phys. Rev. B **14**, 1248 (1976)]. The close agreement between present results and those of Chang and co-workers [Phys. Rev. Lett. **37**, 1581 (1976); Phys. Rev. A **19**, 866 (1979)] reconfirms that the binary liquid and the Ising model belong to the same universality class and also confirms the validity of the present procedure.

I. INTRODUCTION

It has been known that the results from scattering studies of the equilibrium properties of a fluid and a binary liquid mixture near their critical points agree within experimental uncertainty with the predictions of scaling theories.¹ Recent small-angle x-ray scattering experiments have shown that the correlation scaling function can no longer be represented by a simple scaling law without corrections.² On the contrary, light scattering studies have provided no evidence for correction-to-scaling contributions in the correlation scaling function.³ These experimental results, which apparently conflict, result from the differences in the two methods used for the determination of the critical exponent η and of the correlation scaling function from the scattering data, where η is a measure of the extent to which the actual correlation function differs from the classical behavior predicted by the Ornstein-Zernike theory.⁴ For the determination of η and the correlation scaling function, it is desirable to probe the region of large $Q\xi$ with substantial accuracy, where Q is the scattering vector ($=4\pi\sin\theta/\lambda$, λ is the wavelength, 2θ is the scattering angle) and ξ is the correlation length. This region is entered by making either Q or ξ large. The former is accessible with x-ray and neutron small-angle scattering, while the latter is accessible with light scattering. A very careful light scattering study of the correlation function near the critical point of a binary liquid mixture has been reported, where problems occurring at large ξ , such as multiple-scattering and gravitational effects, were minimized.³ On the other hand, the experimental results obtained by small-angle scattering studies are still marred by distortions produced by the instrumental effects. Therefore, substantial improvements in the experimental techniques have been needed to clarify the details of the corrections.

In the present paper, we present a new method of evaluating η and the correlation scaling function of a binary liquid mixture using small-angle x-ray scattering.

We made an effort to obtain high-precision experimental data. First we chose a system amenable to the x-ray studies, the binary liquid mixture of perfluoromethyl-cyclohexane and *n*-heptane, which has a large difference in electron densities between the two components and a reasonably low absorption coefficient. This is one of the best systems from the viewpoint of x-ray contrast. Second we have performed the scattering experiments under infinite slit collimation. Accordingly, theoretical equations derived for infinite slit collimation have been employed in the actual data analysis to exclude various uncertainties accompanied by the slit-collimation correction. Third we used molybdenum radiation instead of the usual copper radiation, by which a drastic improvement of the x-ray sample cell has been made; i.e., the sample cell has a uniform and precisely measurable size and is an interchangeable cell in the strictest sense. Last a reasonable background correction was applied to analyze the experimental data, which permitted us to neglect the effects of the cross-section factor. These measures enabled us to determine the first precise correlation scaling function from small-angle x-ray scattering measurements.⁵

II. EXPERIMENTAL

Reagent-grade perfluoromethyl-cyclohexane was purified by passing it through a 1-m long, 8-mm-diam column packed with silica gel. The treated solvent was fractionally distilled in a nitrogen atmosphere. Reagent-grade *n*-heptane was fractionally distilled over metal sodium in a nitrogen atmosphere. The purity of these solvents was at least 99.99 mole %. The preparation of the solution was performed in a dry box under nitrogen. A detailed description of the sample preparation procedures has been reported elsewhere.⁶ We paid particular attention to avoiding moisture in the air.

Since the precise value of the critical point for perfluoromethyl-cyclohexane-*n*-heptane has not been re-

ported, we tried to determine the critical point by the phase-equilibrium measurements. The system has an upper critical point. The critical point ($T_c = 26.38^\circ\text{C}$, $\phi_{1c} = 0.488$) was established by the coexistence curve and the diameter, where ϕ_{1c} is the volume fraction of perfluoromethyl-cyclohexane. Although the same sample was used for the small-angle x-ray scattering experiments, it showed the critical point ($T_c = 26.35^\circ\text{C}$, $\phi_{1c} = 0.488$). This is slightly different from the critical temperature determined by phase-equilibrium measurements. The slight difference between these critical temperatures is attributed to differences of thermostated baths and temperature detection employed in the two measurements.

The sample cell consisted of a 85-mm-long pyrex tube with internal and external diameters of 4.15 ± 0.01 mm and 4.75 ± 0.01 mm, respectively. The cell was specially manufactured by Shigemi Standard Joint Industrial Company. It was filled with a sample of critical composition and was frozen and sealed with a torch under vacuum. The cell was inserted into a thermostated brass block with openings only large enough to allow passage of the x-ray beam and exit of the scattered radiation. These openings were covered with aluminum foil (thickness $15 \mu\text{m}$) and the surroundings of the cell were evacuated. The sample cell and the sample holding block are shown in Fig. 1. The sample holding block was thermostated by circulating water from a constant temperature bath. A chromel-alumel thermocouple was inserted in a hole near the cell on the block which indicated a constant temperature within 0.01°C . The thermocouple was calibrated by a HP Model 2804A quartz thermometer.

The scattering system and equipment for measurement were almost the same as those reported previously except for the following points.⁷ The x-ray source was a

Toshiba's line-focus molybdenum target tube operated from Rigaku Denki x-ray generator (D-10C type) at an average potential of 37.5 kV and an average current of 22 mA and the x-ray intensity was detected by a scintillation counter. The monochromatization was accomplished by a pulse height analyzer with a Zr filter to separate the Mo $K\alpha$ line. The intensity fluctuation of the x-ray source was measured repeatedly using a pure solvent at a fixed angle.

The collimation system employed was a modified Kratky small-angle camera made by Rigaku Denki Company. The Kratky camera was set in order to fulfill the conditions required by infinite slit collimation. The infinite slit condition in our present collimation was satisfied within the scattering angle of 2.0° , whose angle was evaluated from the knowledge of the weighting function calculated according to Hendricks and Schmidt⁸ and was confirmed using the measured weighting function.⁹ Since it is known that termination errors can be appreciable for the infinite slit collimation, particularly for intensity functions like the Lorentzian curve which decreases relatively slowly as the scattering angle increases,¹⁰ we no longer corrected the measured intensity. Instead, we tried to transform the theoretical equations for point collimation into the corresponding equations for infinite slit collimation. The transformation was made analytically to the Ornstein-Zernike equation,⁴ the Fisher-Langer expansion,¹¹ and numerically to the Bray equation.¹² In the above transformation, the effect for beam width was considered as follows. After interpretation of the data, the experiment was carried out under the slit condition with the thickness of one-half of the original width. The two curves after background correction agreed within the experimental error. Further validity has been obtained by the calculation of the weighting function for the width.

Noting that the scattering intensity observed at the minimum angle is dominated by a parasitic scattering, the data point at the angle was eliminated in a later analysis. The scattering intensities from the empty cell and each solvent have been measured to estimate the background component.

The absorption of the critical sample, the empty sample, and each solvent, which are the same samples as those employed in the scattering measurements, was measured using the Mo $K\alpha$ line monochromatized by the crystal of aluminum at a wide angle.⁷

III. DATA ANALYSIS

The total scattered intensity near the critical point for infinite slit collimation $J_T(Q)$ is separated into a critical component $J_C(Q)$ and a background component $J_B(Q)$,

$$J_T(Q) = J_C(Q) + J_B(Q), \quad (1)$$

respectively. The mathematical relation between $J_C(Q)$ for infinite collimation and $I_c(Q)$ for point collimation is given by¹³

$$J_C(Q) = 2 \int_0^\infty I_c((Q^2 + y^2)^{1/2}) dy. \quad (2)$$

The critical component $I_c(Q)$ is usually represented as a

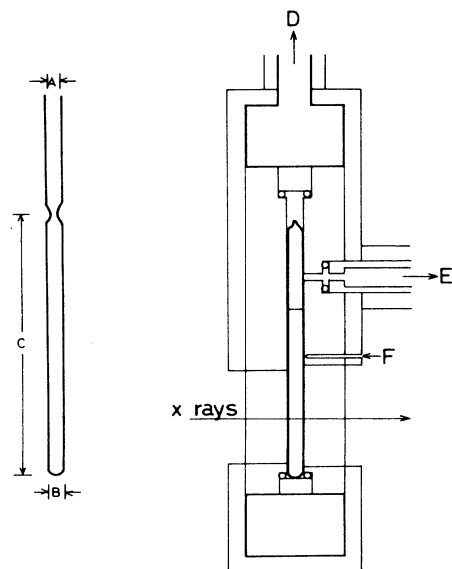


FIG. 1. Sketch of sample cell and sample holding block used in this study: $A = 4.15 \pm 0.01$ mm; $B = 4.75 \pm 0.01$ mm; $C = 85$ mm; D , to a constant temperature bath; E , to a vacuum pump; and F , a thermocouple.

product of the form factor of a molecule $\Phi(Q)$ and the structure factor of critical fluctuation $S_c(Q)$, except a proportional constant, i.e.,

$$I_c(Q) = \Phi(Q)S_c(Q), \quad (3)$$

where $S_c(Q) = S_c(0)g_c(Q\xi)$, $S_c(0)$ is $S_c(Q)$ at $Q=0$, and $g_c(Q\xi)$ is the correlation scaling function for point collimation.

In evaluating the $S_c(Q)$ from Eq. (3), it is very important to exclude any effect of the form factor on the $S_c(Q)$. It is noted that in the small-angle scattering experiment, the molecular arrangement around a molecule in interest is approximated by a shell structure first introduced by Belbeoch and Guinier.¹⁴ The concept of shell structure has been developed by Kirste¹⁵ and applied to interpret the experimental data in a polymer solution.^{15,7} The background component is not expressed by J_B but by J_{BX} , in which the J_{BX} represents the function of the electron density. The effect of the form factor $\Phi(Q)$ can be minimized by using this model, that is, the two effects of inner and outer shells are canceled out by changing the electron density in the background component (the condition of contrast matching). Then $\Phi(Q)$ does not depend on the scattering vector, especially in the present small-angle region. Such a molecule with shell structure (an effective molecule) may be considered as a sort of "renormalized particle" in quantum field theory.¹⁶ Furthermore, the condition of contrast matching is confirmed by checking a systematic deviation from $g_c(Q\xi)$ which appeared in the plot of a correlation scaling function obtained from the experiment $g_{CX}(Q\xi, Qa_{\text{eff}})$ against $Q\xi$, where a_{eff} is the size of the effective molecule. The structure factor $S_{CX}(Q, a_{\text{eff}}, \xi)$ is then represented by

$$S_{CX}(Q, a_{\text{eff}}, \xi) = S_c(0)g_{CX}(Q\xi, Qa_{\text{eff}}). \quad (4)$$

In the condition of contrast matching, Eq. (4) is reduced to

$$S_{CX}(Q, a_{\text{eff}} \rightarrow 0, \xi) = S_c(0)g_{CX}(Q\xi, Qa_{\text{eff}} \rightarrow 0), \quad (4')$$

and then $g_{CX}(Q\xi, Qa_{\text{eff}} \rightarrow 0)$ is reduced to $g_c(Q\xi)$.

$$g_{\text{Bray}}^{-1}(x) = 1 + x^2(1 + x^2/9)^{-7/2} \{1 + \eta[s_2(x) - (w/2)\ln(1 + x^2/9)/(1 + x^2/36)]\},$$

with

$$s_2(x) = (x^2/9) \int_1^\infty du [1 - F(u)] / [u(u^2 + x^2/9)].$$

Here w is a parameter restricted to the range $-1/7 \leq w \leq 1$ and $F(u)$ is the spectral function, truncated so as to vanish for $u < 2$,¹² which is derived from the Fisher-Langer expansion

$$g_{\text{FL}}(x) = (C_1/x^{2-\eta})(1 + C_2/x^{(1-\alpha)/\nu} + C_3/x^{1/\nu} + \dots) \quad (x \gg 1) \quad (8')$$

In the present analysis, the background component J_{BX} was evaluated from the following equation by assuming the additivity of intensities and neglecting the cross terms:¹⁷

$$J_{BX} = v_{XC}J_X + (1 - v_{XC})J_G, \quad (5)$$

where v_{XC} is the volume fraction of component X at the critical composition, the subscripts $X=G, 1$ and 2 represent the glass tube, perfluoromethyl-cyclohexane, and n -heptane, respectively. By changing the combination of these components, we obtained J_{B2} as the background component which agreed with the above condition of contrast matching. Under the condition, the correlation scaling function for infinite collimation \bar{g}_{C2} is given by

$$\bar{g}_{C2}(Q\xi) = J_{c2}(Q)/J_{c2}(0). \quad (6)$$

The correlation scaling function \bar{g}_{C2} agrees with the following equations in the boundary conditions:^{4,11}

$$\bar{g}_{\text{OZ}}(x) = 1(1 + x^2)^{1/2} \quad (x \ll 1) \quad (7)$$

$$\bar{g}_{\text{FL}}(x) = (\bar{C}_1/x^{(1-\eta)})(1 + \bar{C}_2/x^{(1-\alpha)/\nu} + \bar{C}_3/x^{1/\nu} + \dots) \quad (x \gg 1) \quad (8)$$

where $x = Q\xi$,

$$\begin{aligned} \bar{C}_1 &= \frac{C_1 \sqrt{\pi} \Gamma((1-\eta)/2)}{C_0 \Gamma(1-\eta/2)}, \\ \bar{C}_2 &= \frac{C_2 \Gamma((1-\eta)/2) \Gamma([1-\eta+(1-\alpha)/\nu]/2)}{\Gamma(1-\eta/2) \Gamma(1-\eta/2+(1-\alpha)/2\nu)}, \\ \bar{C}_3 &= \frac{C_3 \Gamma((1-\eta)/2) \Gamma((1-\eta+1/\nu)/2)}{\Gamma((1-\eta)/2) \Gamma(1-(\eta-1/\nu)/2)}, \end{aligned} \quad (9)$$

$C_0 = 3.1784$, $C_1 = 0.962$, $C_2 = 1.773$, $C_3 = -2.745$, and α and ν are the critical exponents of specific heat and correlation length, respectively. In order to interpret experimental data of any values of x , the correlation scaling function proposed by Bray¹² was numerically integrated,

$$\bar{g}_{\text{Bray}}(x) = \int_0^\infty g_{\text{Bray}}[(x^2 + \xi^2 y^2)^{1/2}] dy / \int_0^\infty g_{\text{Bray}}(\xi y) dy, \quad (10)$$

where

through the relation

$$\text{Im} g_{\text{FL}}^{-1}(i|x|) = \frac{\sin(\pi\eta/2)/C_1}{|x|^{2-\eta} F(|x|/3)}.$$

IV. RESULTS AND DISCUSSION

The scattering curves after the correction of the sample transmission and the background component are shown

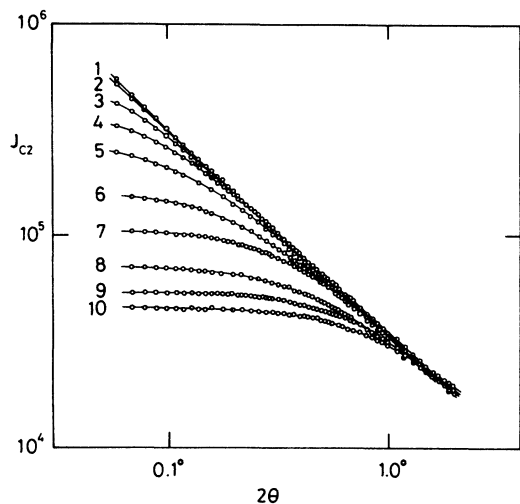


FIG. 2. Scattering curves, corrected for background scattering, for the binary mixture of perfluoromethyl-cyclohexane and *n*-heptane: 1, $t = 3.672 \times 10^{-4}$; 2, 5.676×10^{-4} ; 3, 1.603×10^{-3} ; 4, 3.539×10^{-3} ; 5, 6.844×10^{-3} ; 6, 1.536×10^{-2} ; 7, 3.628×10^{-2} ; 8, 6.056×10^{-2} ; 9, 9.819×10^{-2} ; and 10, 1.243×10^{-1} .

in Fig. 2. The scattering curves numbered 1–10 represent the values of the reduced temperature difference t , where t is $(T - T_c)/T_c$ and T_c is the critical temperature. Taking into account of the temperature range in which a simple power law is applicable, only seven curves (1–7) are analyzed in the present paper. The background scattering from the empty cell is then smaller than 6% of the total intensity. Noting that \bar{g}_{C2} is represented by Eq. (7) in the limit of $Q \rightarrow 0$, the correlation length ξ_2 and the scattering intensity at $Q \rightarrow 0$, $J_{C2}(0)$ were evaluated from the slope and the ordinate of the scattering curves numbered 3–7 using the

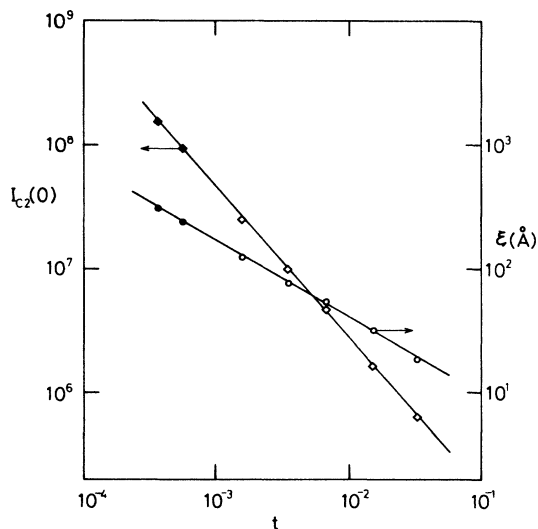


FIG. 3. Double logarithmic plot of the correlation length and the scattering intensity at the scattering vector $Q = 0$ vs the reduced temperature difference $t = (T - T_c)/T_c$.

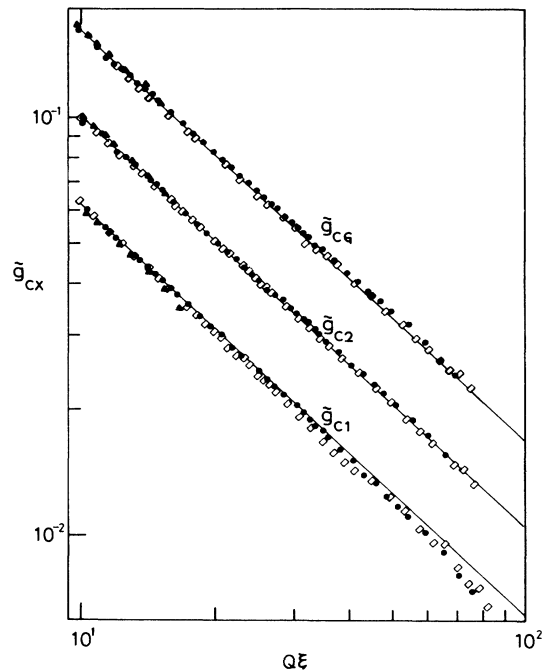


FIG. 4. Double logarithmic plot of the experimental correlation scaling function $\bar{g}_{CX}(Q\xi)$ vs $Q\xi$ restricted to $Q\xi \geq 10$. The solid line represents the Fisher-Langer equation [see Eq. (8) in text] fitted to the data. For further details see text.

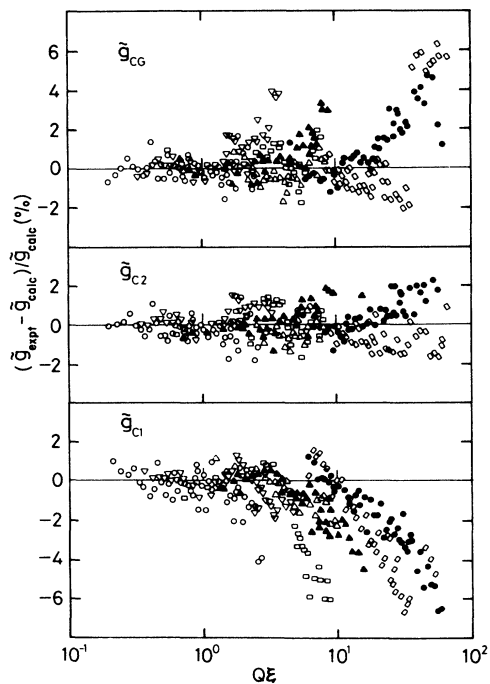


FIG. 5. Plot of the deviations $(\bar{g}_{\text{expt}} - \bar{g}_{\text{calc}})/\bar{g}_{\text{calc}}$ in (%) as a function of the scaling variable $Q\xi$. \bar{g}_{calc} represents the Bray equation with $\nu = \frac{5}{8}$, $\alpha = \frac{1}{8}$, $\eta = \frac{1}{54}$, $c_0 = 3.1784$, $c_1 = 0.962$, $c_2 = 1.773$, and $c_3 = -2.745$.

Ornstein-Zernike equation, where the data analysis was made in the range of $Q\xi < 3$. Because the data points numbered 1 and 2 do not agree with this condition, we evaluated the values of ξ_2 and $J_{C_2}(0)$ for Nos. 1 and 2 by using those obtained from the scattering curves numbered 3–7 and by assuming a simple power law. In this paper we adopted the convention of quoting as error two standard deviations which included the effect of systematic differences between data points of different scattering curves. To obtain the critical exponent values for ξ_2 and $I_{C_2}(0)$, seven data points can be fitted to the formulas

$$\xi_2 = \xi_{20} t^{-\nu}$$

and

$$I_{C_2}(0) = I_{C_{20}} t^{-\gamma},$$

where the values of $I_{C_2}(0)$ were calculated from the relation of $I_{C_2}(0) = \xi_2 J_{C_2}(0) / \pi$. The relationships between ξ_2 and $I_{C_2}(0)$ against t are shown in Fig. 3. We thus obtain

$$\xi_2 = (2.33 \pm 0.11) t^{-0.622 \pm 0.01}$$

and

$$I_{C_2}(0) = (9.94 \pm 0.49) \times 10^3 t^{-1.22 \pm 0.02}.$$

The results verify that the critical exponent values of ν and γ agree with the values calculated theoretically for the Landau-Ginzburg-Wilson model within the experimental uncertainty. Furthermore, these values do not depend on the subtraction method. Using the Fisher relation of $\gamma = (2 - \eta)\nu$, we obtain $\eta = 0.03(2) \pm 0.03(2)$. Although the value of η determined in this way can be quite sensitive to uncertainties in other exponents employed in the calculation, our work shows η to be definitely smaller than the values of 0.11 ± 0.03 ,¹⁸ 0.07 ± 0.01 ,² 0.09 ± 0.02 ,¹⁹ and $0.085(8) \pm 0.026(3)$ (Ref. 20), without corrections previously reported for fluids and binary mixtures in the neutron and x-ray small-angle scattering experiments and being close to the best value of 0.017 ± 0.015 reported for a binary mixture in the light scattering experiment.³

In order to examine the condition of the contrast matching and to the more direct determination of η , a double logarithmic plot of \bar{g}_{CX} versus $Q\xi$ is shown in Fig. 4 for the different subtraction methods. The solid curves in Fig. 4 are the scattering curves calculated from the Fisher-Langer expansion of Eq. (8), where $\nu = \frac{5}{8}$, $\alpha = \frac{1}{8}$, and $\eta = \frac{1}{54}$ are employed as the critical exponent values.^{3,12} The best fit to this equation is found in \bar{g}_{C_2}

and an upward deviation from Eq. (8) is observed in \bar{g}_{CG} , while a downward deviation from Eq. (8) is observed in \bar{g}_{C_1} . It is seen that the values of η almost equals $\frac{1}{54}$. Furthermore, it is important to note that the data points for \bar{g}_{C_1} and \bar{g}_{CG} are considerably scattered in comparison with those for \bar{g}_{C_2} , and the origin for the scattered data is explained by taking into account of the shell structure around each molecule. That is, the downward scattering data for \bar{g}_{C_1} stem from the downward deviation of $\Phi_1(Q)$ at each t from $\Phi_1(Q) = 1$, where the cross-section factor $\Phi_1(Q)$ is almost dominated by the outer shell, while data for \bar{g}_{CG} stem from the upward deviation of $\Phi_G(Q)$ at each t from $\Phi_G(Q) = 1$, where $\Phi_G(Q)$ is dominated by the inner shell. In the present case, it is easily seen that the condition of the contrast matching is realized in \bar{g}_{C_2} in the Q range investigated.

It is further worthwhile to compare present results with a more general correlation scaling function. As the more general scaling function, the correlation scaling function proposed by Bray was selected because the function contains Eqs. (7) and (8) as the boundary conditions and the extensive experimental verification of this function have been already given by the light scattering method.³ These results are shown in Fig. 5. It is noted that no systematic deviation of the experimental data from the calculated values was observed in the plot of deviations $(\bar{g}_{C_2} - \bar{g}_{\text{calc}}) / \bar{g}_{\text{calc}}$ vs $Q\xi$, while an upward deviation was observed in the plot of $(\bar{g}_{CG} - \bar{g}_{\text{calc}}) / \bar{g}_{\text{calc}}$ and a downward deviation was obtained in the plot of $(\bar{g}_{C_1} - \bar{g}_{\text{calc}}) / \bar{g}_{\text{calc}}$. These results provide further verification of the application of the model of shell structure to the evaluation of the cross-section factor. A preliminary analysis with the critical exponents fixed at their best known values²¹ gave equally satisfactory representations of the experimental scattering data.

In conclusion, the present procedure cross checks the finding that binary liquids and the Ising model belong to the same universality class without any correction-to-scaling contributions in the correlation scaling function. The procedure, never before suggested, thus has the benefit that is free from the uncertainties in collimation corrections, the effects of the cross-section factor, and the cell size used.

ACKNOWLEDGMENTS

The author is indebted to Professor Y. Miyake for reading the manuscript. Calculations were carried out on the HITAC M262H computer of the Computer Center of Hokkaido University.

¹M. E. Fisher, J. Math. Phys. **5**, 944 (1964); M. E. Fisher and A. Aharony, Phys. Rev. B **7**, 2818 (1974).

²E. Gürmen, M. Chandrasekhar, P. E. Chumbley, H. D. Bale, D. A. Doljci, J. S. Lin, and P. W. Schmidt, Phys. Rev. A **22**, 170 (1980).

³R. F. Chang, H. Burstyn, J. V. Sengers, and A. J. Bray, Phys. Rev. Lett. **37**, 1581 (1976); R. F. Chang, H. Burstyn, and J. V. Sengers, Phys. Rev. A **19**, 866 (1979).

⁴L. S. Ornstein and F. Zernike, Proc. Acad. Sci. Amsterdam **17**, 793 (1914).

⁵Y. Izumi, E. Asano, and Y. Miyake, Rep. Prog. Polym. Phys. Jpn. **28**, 1 (1985).

⁶Y. Izumi, H. Sawano, and Y. Miyake, Phys. Rev. A **29**, 826 (1984).

⁷Y. Izumi, K. Shinbo, M. Fuji, and Y. Miyake, Colloid Polym. Sci. **256**, 1 (1978).

- ⁸R. W. Hendricks and P. W. Schmidt, *Acta Phys. Austriaca* **37**, 20 (1973).
- ⁹Y. Izumi and Y. Miyake, *J. Cryst. Soc. Jpn.* **21**, 282 (1979).
- ¹⁰F. Hossfeld and G. Maier, *Z. Angew. Phys.* **22**, 145 (1967); P. W. Schmidt, *J. Appl. Crystallogr.* **3**, 137 (1970).
- ¹¹M. E. Fisher and J. S. Langer, *Phys. Rev. Lett.* **20**, 665 (1968).
- ¹²A. J. Bray, *Phys. Lett. A* **55**, 453 (1976); *Phys. Rev. Lett.* **36**, 285 (1976); *Phys. Rev. B* **14**, 1248 (1976).
- ¹³J. W. M. Dumond, *Phys. Rev.* **72**, 83 (1947); A. Guinier and G. Fournet, *Nature (London)* **160**, 501 (1947).
- ¹⁴B. Belbeoch and A. Guinier, *Acta Metall.* **3**, 370 (1955).
- ¹⁵R. G. Kirste, *Z. Phys. Chem. (Neue Folge)* **42**, 351 (1964).
- ¹⁶R. D. Mattuck, *A Guide to Feynman Diagrams in the Many-Body Problem*, (McGraw-Hill, New York, 1976), pp. 5 and 25.
- ¹⁷K. Muller, in *Small Angle X-ray Scattering*, edited by O. Glatter and O. Kratky (Academic, London, 1982), Chap. 7, p. 215.
- ¹⁸V. P. Warkulwitz, B. Mozer, and M. S. Green, *Phys. Rev. Lett.* **32**, 1410 (1974).
- ¹⁹H. Bale, J. S. Lin, D. A. Dolejsi, J. L. Lasteel, O. A. Pringle, and P. W. Schmidt, *Phys. Rev. A* **15**, 2513 (1977).
- ²⁰R. Schneider, L. Belkoura, J. Shelten, D. Woermann, and B. Chu, *Phys. Rev. B* **22**, 5507 (1980).
- ²¹J. V. Sengers and J. M. H. Levelt Sengers, *Ann. Rev. Phys. Chem.* **37**, 189 (1986).